UCID- 20297-85-1

LAWRENCE LIVERMORE NATIONAL LABORATORY
GRANULAR FLOW PROJECT - QUARTERLY REPORT

January - March 1985

Edited by
O.R. Walton

For
U.S. Department of Energy
Office of Fossil Energy
Pittsburgh Energy Technology Center
Pittsburgh, Pennsylvania

March 1985

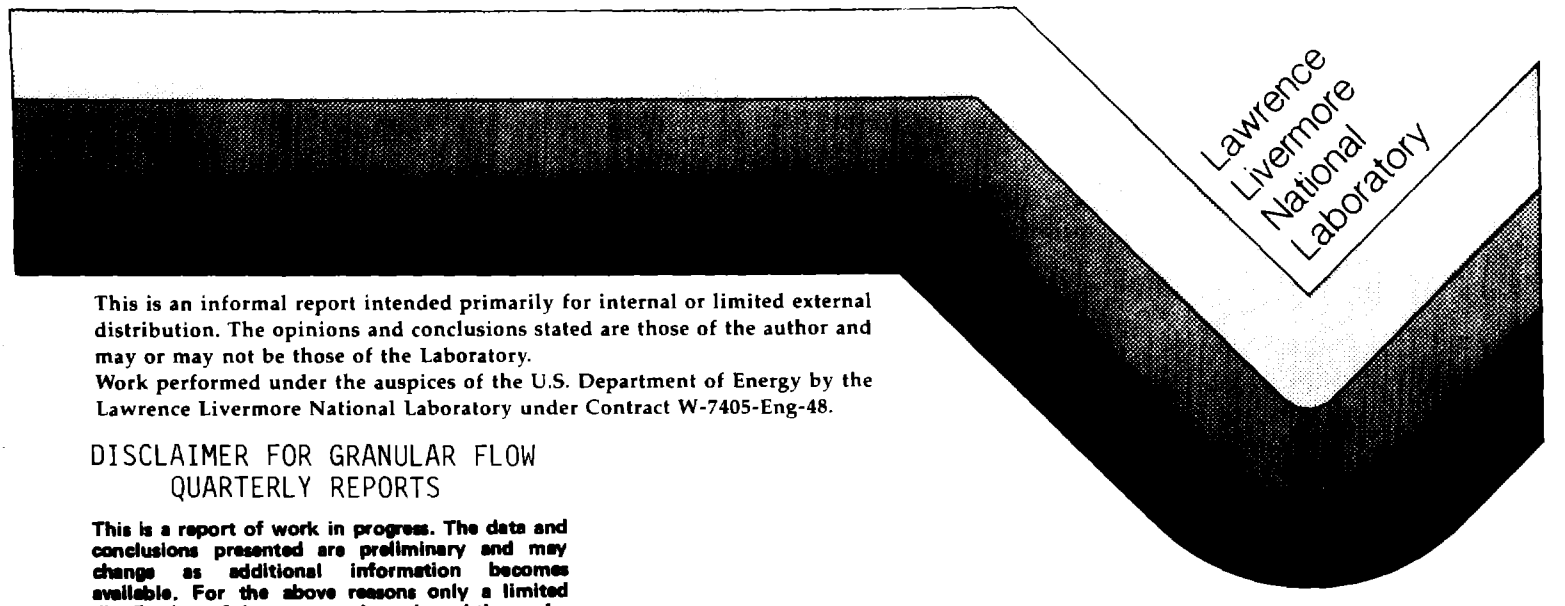

DISCLAIMER FOR GRANULAR FLOW QUARTERLY REPORTS

This is a report of work in progress. The data and conclusions presented are preliminary and may change as additional information becomes available. For the above reasons only a limited distribution of these reports is made and the reader is requested not to quote conclusions or data. Completed results of the research will be published in conventional channels by appropriate authors.

DISCLAIMER

Printed in the United States of America
Available from
National Technical Information Service
U.S. Department of Commerce
5285 Port Royal Road
Springfield, VA 22161
Price: Printed Copy $ Microfiche $3.50

Page Range	Domestic Price	Page Range	Domestic Price
001-025	$ 7.00	326-350	$ 26.50
026-050	8.50	351-375	28.00
051-075	10.00	376-400	29.50
076-100	11.50	401-426	31.00
101-125	13.00	427-450	32.50
126-150	14.50	451-475	34.00
151-175	16.00	476-500	35.50
176-200	17.50	501-525	37.00
201-225	19.00	526-550	38.50
226-250	20.50	551-575	40.00
251-275	22.00	576-600	41.50
276-300	23.50	601-up[1]	
301-325	25.00		

[1]Add 1.50 for each additional 25 page increment, or portion thereof from 601 pages up.

Granular Flow Project Quarterly Report

January - March 1985

Edited by: O.R. Walton

New three-dimensional discrete particle computer models for simulating the flow behavior of granular solids are under development in the Granular Flow project at LLNL. The first steps in developing these models have been an examination of interparticulate force models and the construction of a two-dimensional steady state shearing model to test both numerical methods and diagnostic algorithms. The two orthogonal components of the contact force acting between particles are modeled separately. A new position-dependent inelastic normal-force model was reported last quarter, as well as calculations that verified the numerical methods and averaging techniques used in the new two-dimensional steady-state shearing model. We report below the tangential friction model and initial results from a calculational parameter study of shearing flow in two-dimensions performed during the second quarter of FY85.

Incrementally Slipping Friction Model

The tangential friction force model used in our calculations of colliding particles is patterned after theoretical models for the friction forces acting between elastic spheres in contact, [Mindlin, 1949] and [Mindlin and Deresiewicz, 1953]. Mindlin's expression for the tangential compliance acting during small displacements is based on the assumption that the approximate Hertzian normal stress distribution over the circular area of contact is unaffected by the tangential displacement. The main thrust of his theory is that the outermost annulus of the circular area of contact between two spheres

has very low normal stresses acting on it and will thus experience some slipping for any amount of tangential displacement. The central region of the contact circle, on the other hand, has higher normal stresses and initially experiences an elastic shear deformation before beginning to slip. The radius of the boundary between the slipping annulus and the non-slipping central circle depends on the amount of the displacement. Upon reversal of the direction of tangential motion, a new annular slip region starts at the outer radius of the contact circle while the innermost circle merely unloads elastically. Mindlin's theoretical analysis obtained by integrating over the stressed area of contact reduces to relatively simple analytic expressions for the effective incremental stiffness of a non-linear tangential spring, K_T, given by

$$K_T = K_o \left(1 - \frac{T}{\mu N}\right)^{1/3} \tag{1}$$

for the initial loading, and by

$$K_T^* = K_o \left(1 - \frac{T^*-T}{2\mu N}\right)^{1/3} \tag{2}$$

for subsequent unloading.

where: $K_o = K_n \frac{2(1-\nu')}{(2-\nu')}$ = initial tangential stiffness

K_n = effective normal stiffness at this normal load (depends on radii of spheres, elastic constants and displacement in the normal direction.

N = total normal force

μ = coefficient of friction

T = Total tangential force

ν' = Poisson's ratio for the material

T^* = Tangential force at time of direction reversal

The incremental stiffness, K_T, given by equations (1) and (2) starts out at a value of K_o and then monotonically decreases to zero with increasing displacement as the total tangential force, T, approaches the friction limit, μN. Mindlin's theory further predicts that subsequent reloading would have an incremental stiffness, K_T^{**}, and a following unloading would have a stiffness, K_T^{***} given by,

$$K_T^{**} = K_o \left(1 - \frac{T-T^{**}}{2\mu N}\right)^{1/3} \tag{3}$$

$$K_T^{***} = K_o \left(1 - \frac{T^{***}-T}{2\mu N}\right)^{1/3} \tag{4}$$

where T^{**} and T^{***} are the minimum value of T before reloading and the maximum value of T before second unloading, respectively. In order to exactly implement Mindlin's friction expressions in our computer model, we would need to store the value of each successive turning point, T^*, T^{**}, T^{***}...etc. If two particles remain in contact with an oscillating tangential displacement, such a scheme could require large quantities of computer memory and complex bookkeeping logic. We have, instead, employed functions that approximate the expressions of Mindlin (they can correspond exactly to Mindlin's for initial loading and for the first part of the first tangential unloading). Our expression for K_T is given by

$$K_T = \begin{cases} K_o \left(1 - \dfrac{T-T^*}{\mu N-T^*}\right)^{\gamma} & \text{for slip in one direction (T increasing)} \\ K_o \left(1 - \dfrac{T^*-T}{\mu N+T^*}\right)^{\gamma} & \text{for slip in the other direction (T decreasing)} \end{cases} \tag{5}$$

where T^* is initially zero and is subsequently set to the value of total tangential force, T, at the point where the relative tangential slip reverses direction, and γ is a constant nominally set to 1/3 but with other non-negative values allowed. If the normal force changes then the value of T^* in the above expressions is scaled in proportion to the change in the normal force, N.

On each explicit time step of our finite difference calculation a new tangential force, T', is calculated incrementally from the old value of the tangential force, T, the effective tangential stiffness, K_T, and the amount of relative surface displacement between the contacting particles, ΔS, by the expression

$$T' = T + K_T \Delta S \tag{6}$$

with K_T given by equation (5). Thus, in order to calculate the total tangential force acting between each pair of particles, we need to keep only two quantities, T and T^* from one time step to the next.

Figure 1 shows the tangential force vs. tangential displacement as generated by equations (5) and (6) for a series of ever increasing amplitude oscillations of the relative tangential surface displacement, S, with a constant normal force, N, and an exponent $\gamma = 1/3$. If the exponent, γ, is set to zero this model will become a linear tangential spring with stiffness $K_T = K_o$ acting up to the friction limit, μN. If the exponent is made larger than 1/3 the deviation from the initial slope occurs earlier and the approach to the friction limit is more gradual than that shown in Figure 1. Experimental measurements of initial displacements of frictional forces acting between metals in contact (non-spherical bodies) produce force deflection curves that are qualitatively quite similar to the model curve of Figure 1 [for example see Oden and Martins, 1984], but with a more gradual change

in slope, as would be produced with a larger value for the exponent, γ, in our model. Variation of the exponent, γ, then allows us to approximate a range of realistic tangential force vs. displacement behaviors with varying degrees of hystereses and realistic tangential stiffnesses. We are currently working on extensions of this model for contacts between three-dimensional objects where the friction force and the tangential displacement are not necessarily co-linear.

Initial Calculations of Steady State Shearing in Two-Dimensions

We are conducting a series of calculations on the shearing behavior of two-dimensional granular solids consisting of assemblies of inelastic, frictional disks. Periodic boundaries are employed on all four sides of the primary calculational cell. The image cells above and below the primary cell move to the right and left respectively creating a layered shearing structure. Figure 2 shows the primary calculational cell and the nearest moving periodic image cells, with one particle and its various periodic images. Within the cell (and each image cell) a uniform shearing algorithm [after Hoover 1982 and Hoover et al. 1980] is employed ostensively to insure that the shearing field is uniform throughout the cell and does not come just from the motion of the image cells. An extra force proportional to the strain rate and a particle's y-velocity is applied to each particle in the system. This causes free flight trajectories to be curved paths such that a particle's velocity, v_{xi}, relative to the shearing field velocity, u, is a constant. The equations-of-motion use a total x-direction force, F_{xi}, consisting of two terms

$$F_{xi} = \sum_{j \neq i} F_{xij} + m_i \dot{\epsilon} v_{yi} , \qquad (7)$$

one due to the interaction forces between the ith particle and all other particles and one due to the shearing force field.

In typical non-equilibrium molecular-dynamics calculations of steady-state shearing a "constant-temperature" algorithm of some kind is employed to remove the energy added to the system by the shearing field (see for example Hoover 1982, or Evans 1981). In our granular material simulations the natural energy losses due to frictional, inelastic collisions provide the energy loss mechanism. We monitor the average translational kinetic energy in the system

$$\langle KE_T \rangle = \left\langle \sum_i \frac{1}{2} m_i \left[(v_{xi} - u)^2 + v_{yi}^2 \right] \right\rangle$$

as a measure of the "granular temperature" and we also determine the cumulative average deviatoric speed of the particles,

$$\langle v \rangle = \left\langle \sqrt{(v_{xi} - u)^2 + v_{yi}^2} \right\rangle ,$$

the average rotational kinetic energy

$$\langle KE_r \rangle = \left\langle \frac{1}{2} I_o \omega^2 \right\rangle ,$$

and the mean rotational velocity of the particles $\langle \underline{\omega} \rangle$.

In our first series of simulations we used a representative two-dimensional granular material consisting of a set of 30 equal size disks in a cell with a solids packing of 0.70. Each particle in the system had a coefficient of surface friction of 0.5 and the coefficient of restitution of interparticulate collisions was 0.80. We varied the shear rate from 1.0 to 10.0 inverse time units and obtained an almost linear dependence of the mean deviatoric particle speed, $\langle v \rangle$, with the shear rate, $\dot{\epsilon}$, as shown in Figure 3. The other measure of the mean translational speed of the particles, $\sqrt{2\langle KE_T \rangle}$

was within 2% of the value for $\langle v \rangle$. The mean scalar rotational speed, $\sqrt{\langle \omega^2 \rangle}$ was within a few percent of the mean translational speed (for particles with a radius of unity). The rotational velocities were nearly symmetrically distributed about zero resulting in a mean (vector) rotational spin, $\langle \underline{\omega} \rangle$, whose magnitude was two orders of magnitude smaller than the mean rotational speed $\sqrt{\langle \omega^2 \rangle}$. Campbell and Gong [1985] have recently reported two-dimensional calculations with perfectly rough particles in which they obtained a mean rotation rate $\underline{\omega}$ approximately equal to half the shearing rate over a range of packing fractions from 0.2 to 0.6. Our values for $\underline{\omega}$ are at least an order of magnitude lower than this. They are so much smaller than the mean scalar rotational speed $\sqrt{\langle \omega^2 \rangle}$ that it is difficult for us to determine with high confidence a good correlation between $\langle \underline{\omega} \rangle$ and strain rate at a packing fraction of 0.70. However, we believe that the major reason for the difference between our results and those of Campbell and Gong is due to the more detailed nature of our tangential interactions. Campbell's tangential interaction has a fixed value for the rotational restitution coefficient, $\beta = 0.0$, independent of the angle of incidence or rotational speeds of the colliding particles. The result of applying our tangential and normal force models is a rotational restitution coefficient that depends on the ratio of the incident tangential surface velocity to incident relative normal velocity as shown in Figure 4, [see Granular Flow Project Quarterly Oct.-Dec. 1984 for a definition of β]. We believe that such a model of tangential interactions is more realistic than choosing $\beta = 0$.

According to the three-dimensional theory of Lun et al. [1984] for inelastic particles without rotation, the dimensionless ratio of the shear rate to the mean particle velocity, $R = \frac{\sigma \dot{\varepsilon}}{\langle v \rangle}$, where σ is the particle diameter, depends only on the coefficient of restitution and the packing fraction, and is independent of the shear rate, $\dot{\varepsilon}$. Our two-dimensional

results, for frictional particles including rotational effects, show a slight decrease in this ratio with increasing shear rate as shown in Figure 5. We have not completed enough of our planned parameters variations to determine how R depends on packing fraction and coefficient of restitution.

In addition to velocity and energy diagnostics we also calculate the cumulative time average of the momentum-flux-density tensor (i.e. the stress tensor) instantaneously given by the expression,

$$\underline{\underline{P}} = \sum_i (\underline{v}_i - \underline{u})(\underline{v}_i - \underline{u}) + \sum_{j>i} \underline{R}_{ij} \underline{F}_{ij} \qquad (8)$$

where the first term is a symmetric dyadic and the second dyadic term contains antisymmetric components if the force between two particles, $\underline{F}_{ij}$, is not parallel to the line joining their centers, $\underline{R}_{ij}$. For short time periods, we did find that $p_{xy} \neq p_{yx}$, however, for all of our steady shearing calculations the cumulative average values of these off diagonal components of the stress tensor were identical to within about a tenth of a percent. Our calculations showed that the effective viscosity, $(p_{xy} + p_{yx})/2\dot{\epsilon}$, varies linearly with the strain rate as shown in Figure 6. This linear variation is consistent with Bagnold's theoretical prediction [1954] that the shear stress should vary as the square of the strain rate under uniform shearing conditions. We also varied the packing fraction, ν, from 0.5 to 0.8 for a 30 particle system undergoing steady-state shearing at a rate $\dot{\epsilon} = 5$ inverse time units. Over most of this range, from $\nu = 0.5$ to $\nu = 0.725$ the material behaved in a fluid-like manner producing an isotropic pressure, $p_{xx} \simeq p_{yy}$. However, at densities higher than $\nu = 0.725$ a single shearing plane developed with the particles forming almost a perfect

crystalline array on either side of this single shear plane. The uniform shearing algorithm with its additional x-direction force, equation (7), did not contribute significantly to any shearing velocity in this crystalline region since the y-velocities were very near zero. The stress ratio p_{xx}/p_{yy} exhibited a discontinuity at the transition from one region to the other (between $\nu = 0.725$ and $\nu = 0.75$) as shown in Figure 7. Also shown in Figure 7 is the ratio of shear to normal stress p_{xy}/p_{yy} (the tangent of the dynamic friction angle tan ϕ_d) as a function of packing fraction, ν. As can be seen from this figure, the dynamic friction coefficient had a nearly constant value of about 0.34 throughout most of the density range dropping slightly to 0.30 when the single shearing plane developed. Note that this dynamic friction coefficient is considerably less than the surface friction coefficient, $\mu = 0.50$, acting between individual particles. In the fluid-like region, $\nu < 0.725$, the granular-temperature varied only a small amount with packing fraction so that the pressure vs. packing fraction curve behaved almost like an isotherm for an "excluded-volume" equation gas. Figure 8 shows the calculated pressure, $P = (p_{xx} + p_{yy})/2$, plotted as a function of packing fraction for the constant shear rate $\dot{\varepsilon} = 5$. Also shown on this figure is the graph of the empirically determined equation,

$$P = \frac{37}{(\frac{1}{\nu}) - (\frac{1}{.77})} \qquad (9)$$

which seems to fit the calculated pressures quite well in the range of ν between 0.50 and 0.725. The precipitous drop in the pressure between $\nu =$ 0.725 and 0.75 is again due to the change in the mode of motion obtained in the calculation, changing from near uniform shearing to a single shear plane in a crystalline solid.

Each component of the stress tensor behaved in a manner very similar to the pressure as evidenced by noting the behavior of the effective viscosity, $(p_{xy} + p_{xy})/2\dot{\epsilon}$, as a function of the packing fraction, shown in Figure 9. Lunn et al [1984] predict for three-dimensional particles, and Campbell and Gong [1985] calculate for perfectly rough, rigid, two-dimensional particles, that the shear stress should go through a minimum and then increase again for packing fractions below about $\nu = 0.40$. We have not done calculations at densities below $\nu = 0.5$ so we cannot corroborate their predictions at this time.

We also calculated and averaged separately both the kinetic and potential parts to the stress tensor (the first and second terms in equation 8, respectively) at each of the several different densities from $\nu = 0.5$ to 0.8 for the fixed shear rate of $\dot{\epsilon} = 5.0$. At the low packing fraction of 0.5 we found that the kinetic (or inertial) term contributed almost 25% of the total pressure and about 13% of the total shear stress. As the density was increased the inertial contribution became a smaller and smaller part of the total until at a density with $\nu = 0.725$ the inertial term was only 5% of the total pressure and only 1.25% of the total shear stress with the collisional (or potential) term dominating all elements of the stress tensor.

In order to learn about the details of the motion being calculated in this initial parameter study, we modified our post-processing plotting routine to generate motion-pictures of the particle positions in the primary calculational cell and in several of the surrounding cells. These moives helped us to identify the phase transition that took place between $\nu = 0.725$ and $\nu = 0.75$. We also ran a series of calculations at the solids packing fraction $\nu = 0.70$ with various numbers of particles (N = 12, 30, 32, and 56)

and in calculational cells with x to y dimensions in ratios of 1:2, 1:1, and 2:1. From these series of calculations we found that the change from fluid-like behavior to a single shearing layer depends to some degree on the size and shape of our calculational cell. Layered shearing is forced at our periodic boundaries but uniform shearing through out the cell will occur if there is significant vibrational energy in the system and thus vertical motion of the particles. The rapid dissipating of energy due to inelastic, frictional collisions limits the distance that the effects of the shearing zone can be propagated through the granular material within each cell. We were able to obtain either a single shearing layer or a nearly uniform shearing behavior at a density of $\nu = 0.70$ by changing the shape of our calculational cell. While we have not completed enough calculations to quantify the thickness of observed "boundary layers" between shearing periodic cells, we are modifying the basic calculational model to include real boundaries on the top and bottom. This real boundary version of the model will not have the artificial shearing force of equation (7) to provide uniform shearing, but will instead, be specifically designed to study the "natural" propagation of energy from moving boundaries into a dissipative granular material. We plan to add additional diagnostics to determine the distributions within the primary calculational cell of several of the calculated quantities such as velocity, density, stress, and energy density. These additional diagnostics will allow us to quickly detect such anomalies as a single shearing plane without having to see movies of the particle positions. The real boundaries, and zonal averaging we are currently adding to this two-dimensional model will also be included in the new three-dimensional model as it is developed.

Summary

We have developed an incrementally-slipping friction model, patterned after theoretical models of frictional contacts, that can produce realistic non-linear friction phenomena. We have incorporated that friction force model in our two-dimensional shearing cell model and have performed a series of calculations of steady state shearing of a single granular material. The shearing cell calculations have verified Bagnold's prediction that shear stress varies as the square of the shear rate for granular solids (even in two-dimensions). The pressure vs. volume behavior we calculate for the granular material at a constant shear rate is quite similar to that of an "excluded-volume" gas at constant temperature. At high densities we find that the granular material in our constant volume calculations tends to form a single shearing layer at the cell boundary with the material inside the cell remaining almost like a crystaline solid. We found that the density at which the transition from uniform shearing to single shearing layer occurs is somewhat dependent on the size and shape of our periodic cell. We are modifying our model to include real boundaries and averaging zones within the calculational cell for material diagnostics.

Publications and Presentations - Jan.-March 1985

Walton, O.R., and Braun, R.L., "Viscosity and Temperature Calculations for Assemblies of Inelastic, Frictional Disks", presented at: 56th Annual Mtg. Soc. of Rheology, Feb. 24-27, 1985, Blacksburg, VA, (UCRL 91756 Abst.)

Walton, O.R., "Utilizing Approximate Frictional Contact Models for Computer Simulation of Block Motion and Granular Material Flow", Interdiciplinary Seminar on Rock Mechanics, Univ. of Calif., Berkeley, March 13, 1985.

References

Bagnold, R. A. (1954), "Experiments on a gravity free dispersion of large solid spheres in a Newtonian fluid under shear," Proc. R. Soc. Lond. A 225, 49-63.

Campbell, C. S. and Gong, A. (1985), "The Stress Tensor in a Two-Dimensional Granular Shear Flow," submitted to J. Fluid Mechanics.

Evans, D. J. (1981), "Non-equilibrium molecular dynamics study of the rheological properties of diatomic liquids," Molecular Physics, Vol. 42, No. 6, 1355-1365.

Hoover, W. G., Evans, D. J., Hickman, R. B., Ladd, A. J. C., Ashurst, W. T., and Moran, B. (1980), "Lennard-Jones triple-point bulk and shear viscosities, Green-Kubo theory, Hamiltonian mechanics, and non-equilibrium molecular dynamics", Phys. Rev. A, 22, pp. 1690-1697.

Hoover, W. G. (1982), "Rheology via non-equilibrium Molecular Dynamics", presented at Society of Rheology Mtg. Evanston, Ill., Oct. 1982, (available as LLNL report UCRL-88315)

Lun, C. K. K., Savage, S. B., Jeffrey, D. J., Chepurning, N. (1984), "Kinetic Theories for Granular Flow: Inelastic Particles in Couette Flow and Slightly Inelastic Particles in a General Flowfield", J. Fluid Mech., Vol. 140, pp223-256.

Mindlin, R. D. (1949), "Compliance of Elastic Bodies in Contact", J. Appl. Mech., Trans ASME, Vol. 71, pp. A-259-268.

Mindlin, R. D. and Deresiewicz, H. (1953), "Elastic Spheres in Contact Under Varying Oblique Forces", J. Appl. Mech., Trans ASME Vol. 20, pp. 327-344.

Oden, J. J. and Martins, J. A. C. (1984), "Models and Computational Methods for Dynamic Friction Phenomena", presented at FENOMECH III, Stuttgart, W. Germany, to appear Computer Methods in Applied Mech. and Eng., North Holland, Amsterdam.

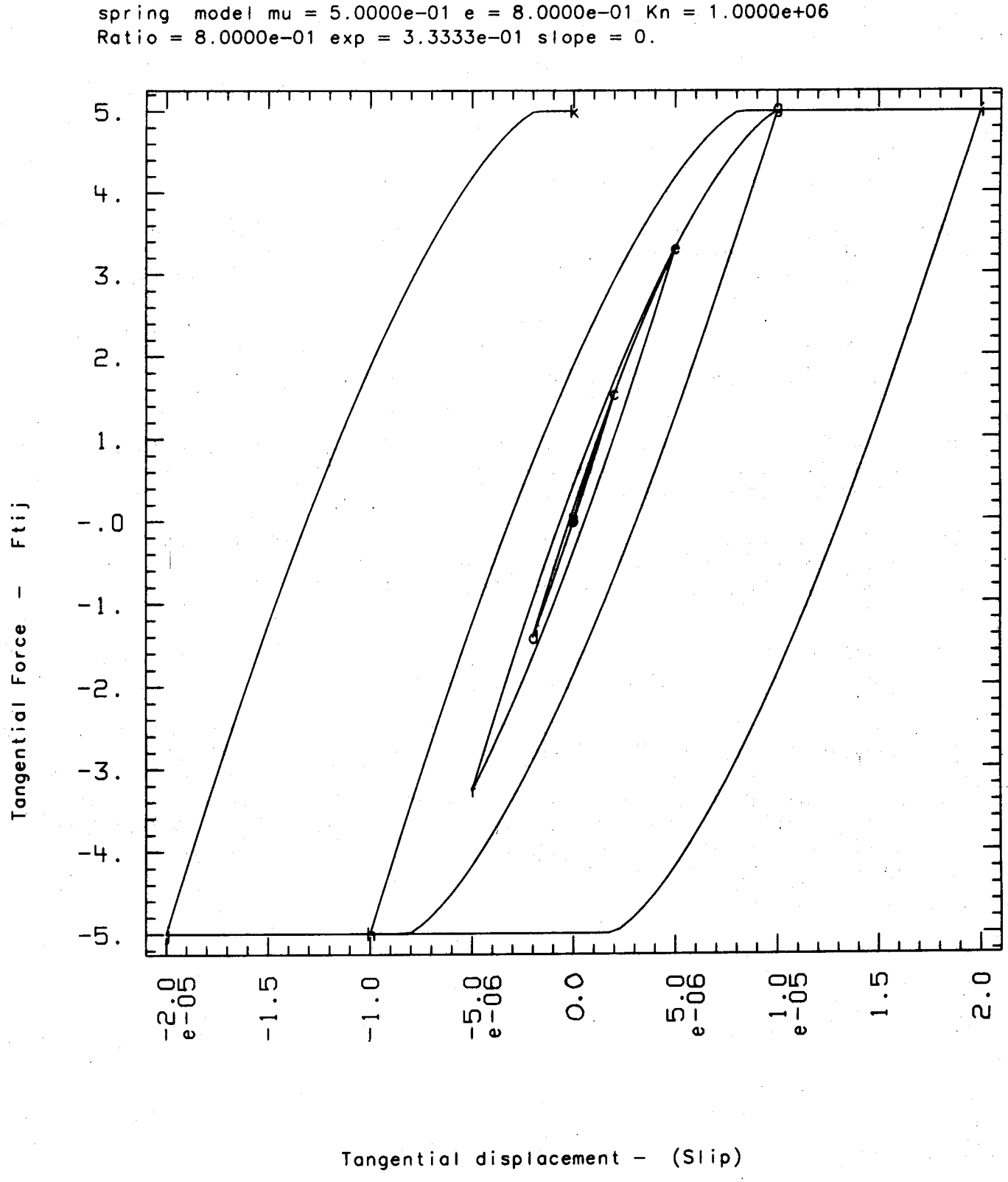

Figure 1. Tangential force vs. displacement as generated by equations (5) and (6) for a series of ever increasing amplitude tangential displacements with constant normal force.

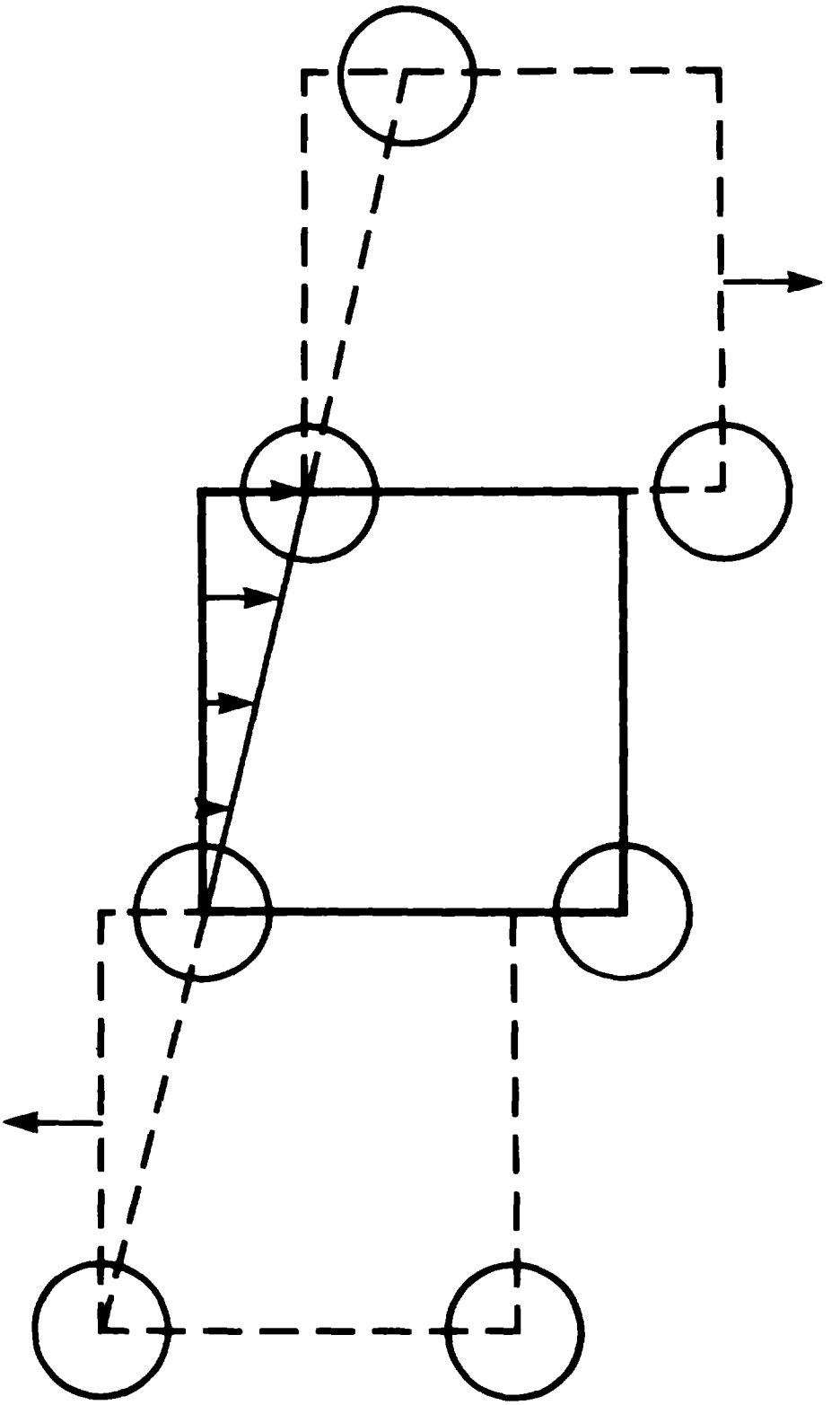

Figure 2. One particle and its images in the stationary primary cell and in the nearest moving periodic image cells.

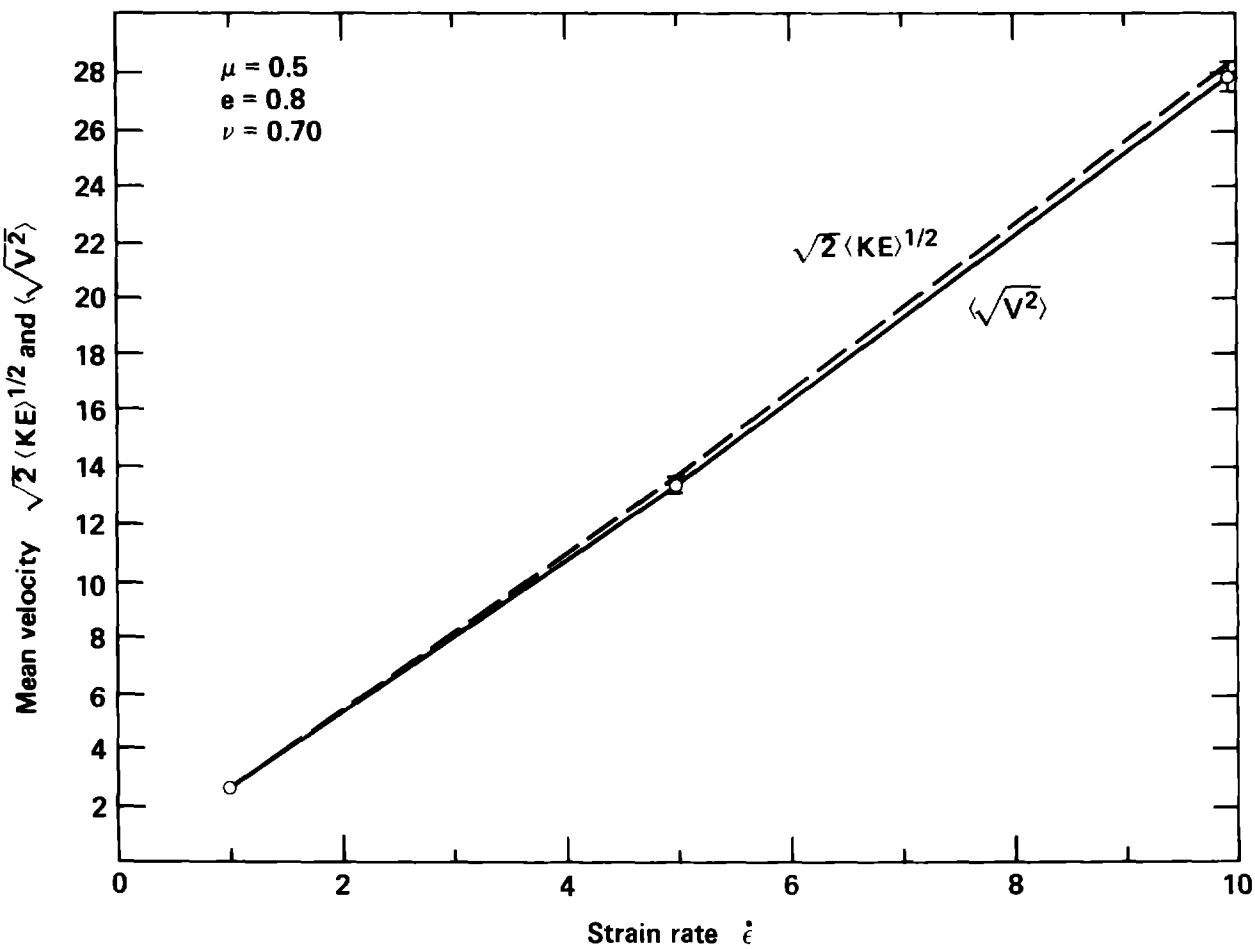

Figure 3. Cumulative average particle velocity vs. shear strain rate for a 30 particle system with solids packing fraction of 0.7, coefficient of restitution 0.8, coefficient of friction 0.5, and ratio of tangential to normal stiffness of 0.80.

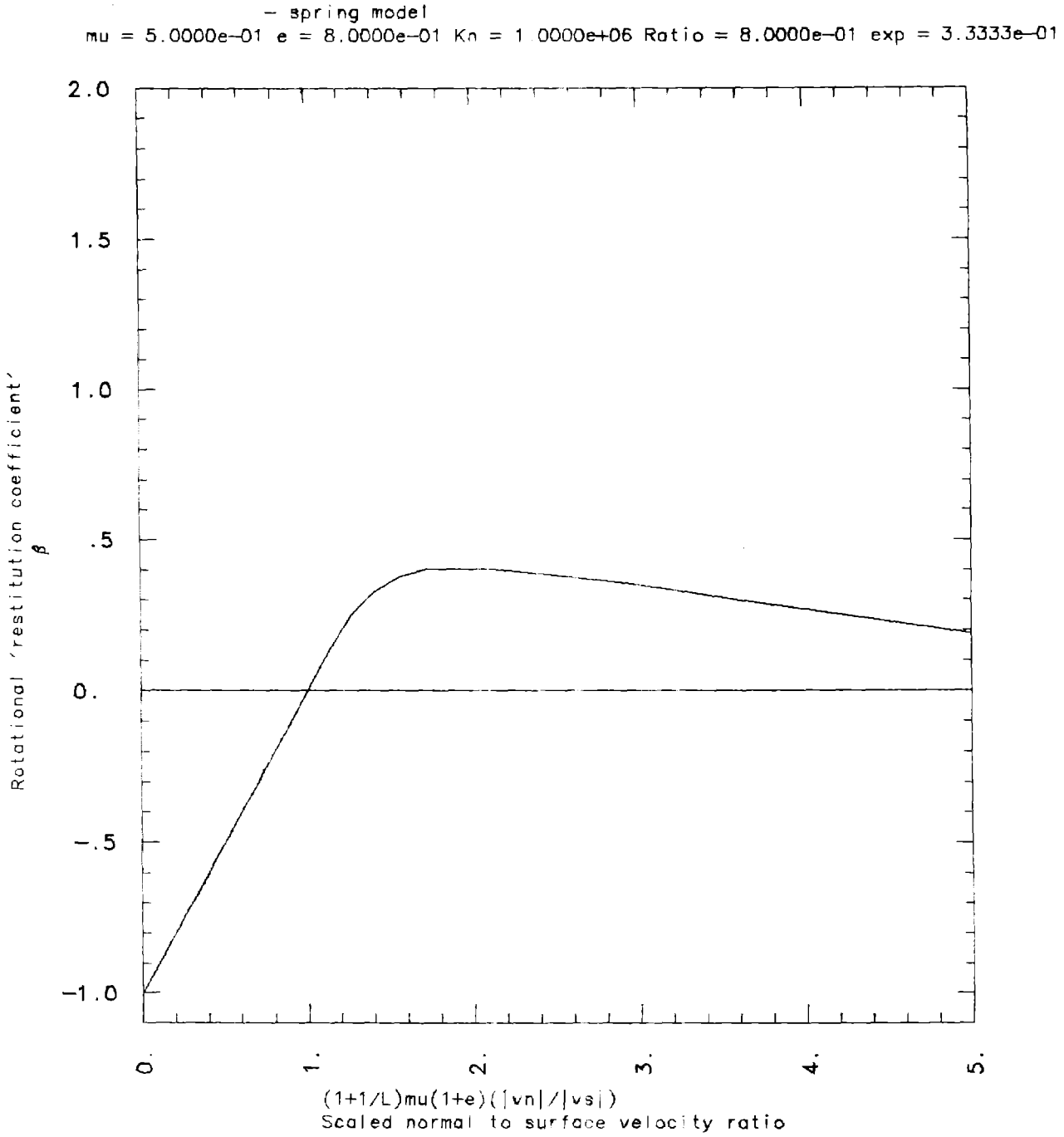

Figure 4. Rotational coefficient of restitution (ratio of initial to final relative tangential velocities) for a two particle collision vs. the tangent of the effective angle of incidence (ratio of the relative surface tangential to normal velocities) as calculated using the incrementally slipping friction model (equation 5) with coefficients of $\nu = 0.5$, $e = 0.8$, $K_N = 1.0 \times 10^6$, $K_o = 0.8 \times 10^6$, $\gamma = 1/3$.

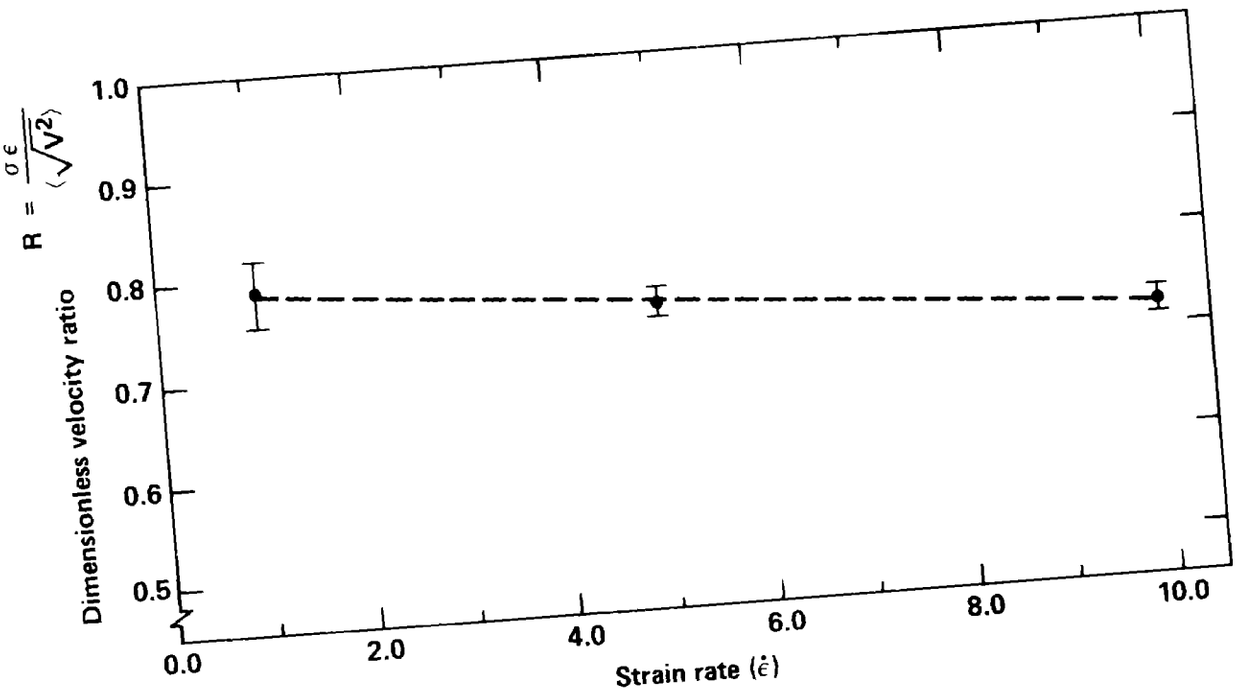

Figure 5. Calculated dimensionless velocity ratio vs. shear strain rate for a 30 particle system at a solids packing fraction of 0.70.

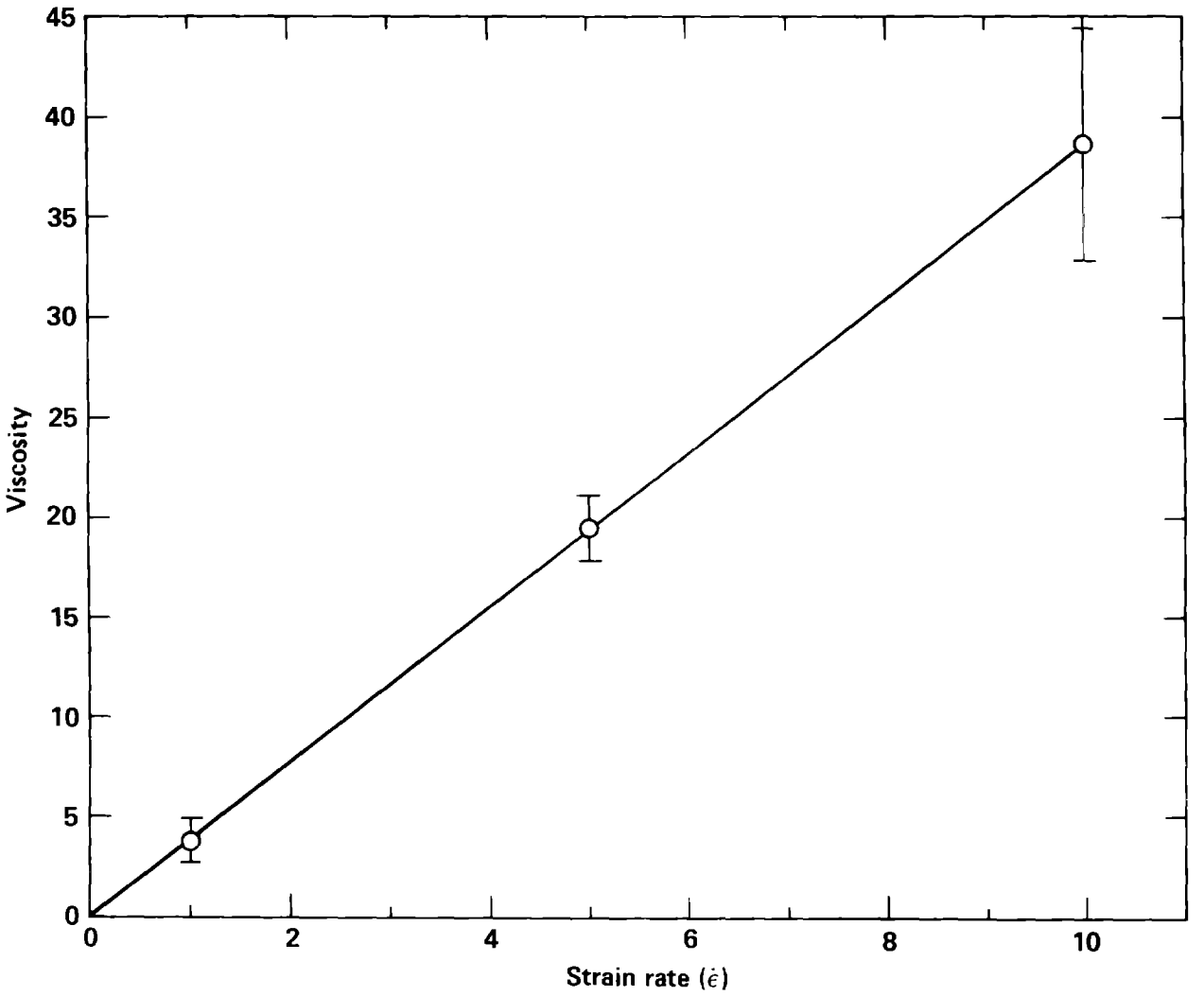

Figure 6. Calculated viscosity vs. shear strain rate for a 30 particle system at a solids packing fraction of 0.70

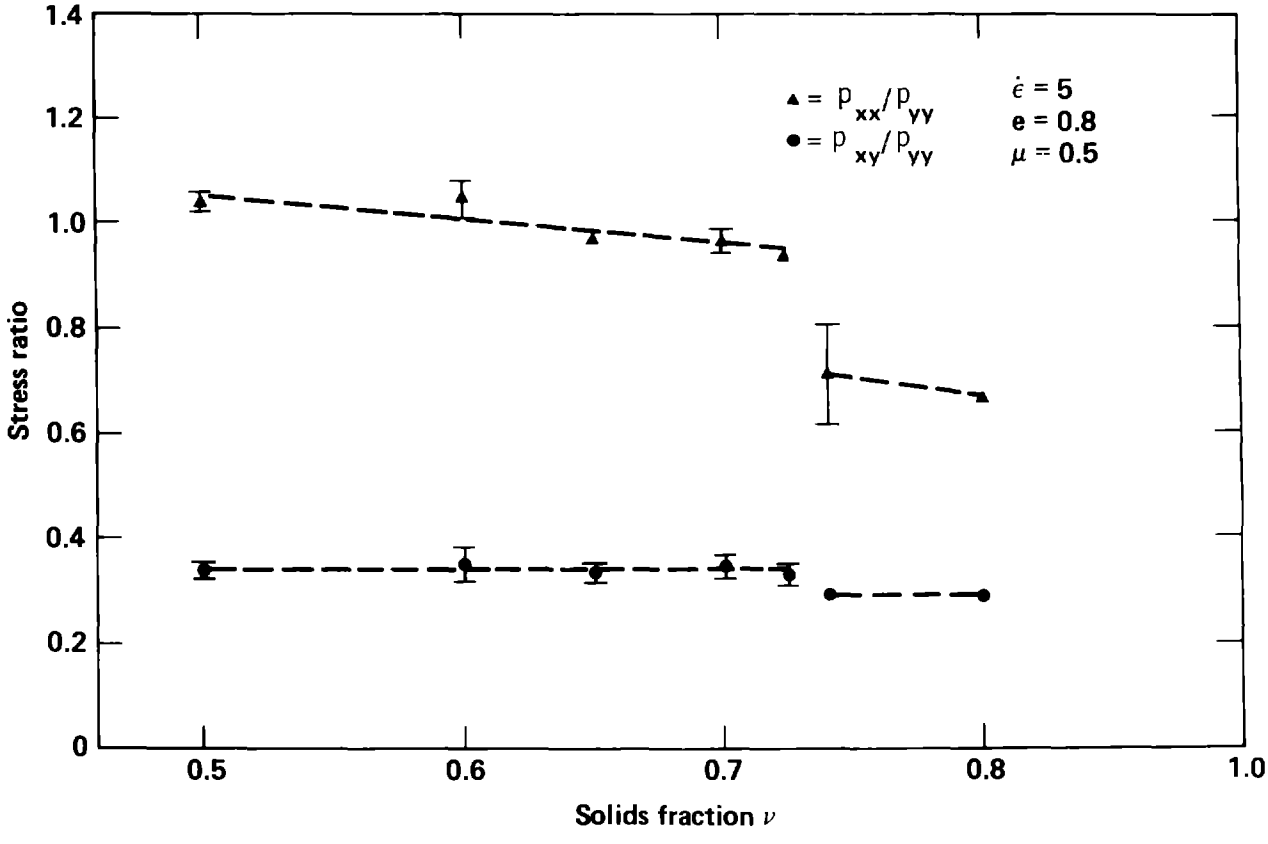

Figure 7. Calculated ratio of stress components p_{xx}/p_{yy} and p_{xy}/p_{yy} as a function of solids packing fraction for a 30 particle systems undergoing steady shearing at a rate of 5 inverse time units.

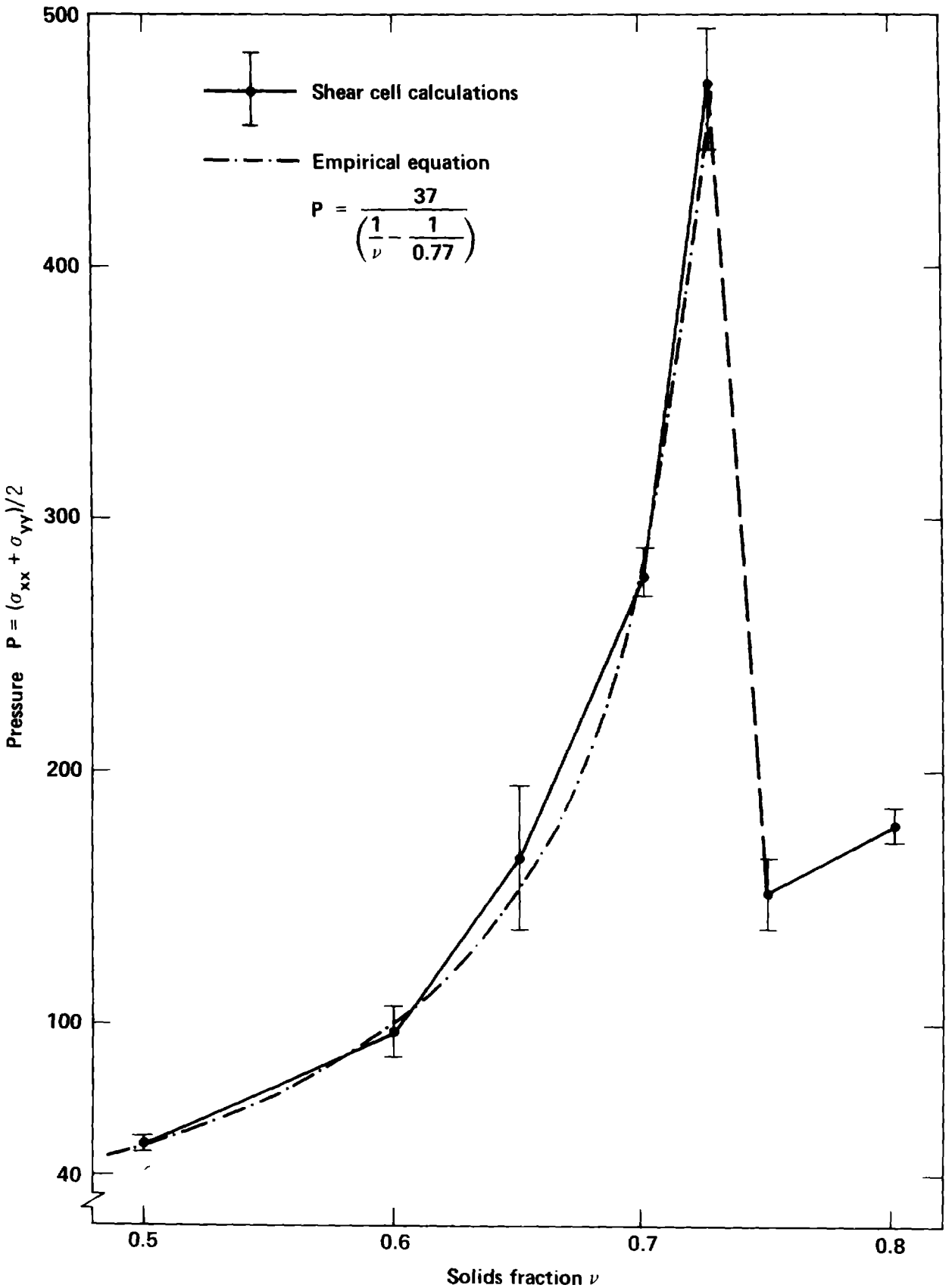

Figure 8. Calculated two-dimensional pressure, $(p_{xx}+p_{yy})/2$, as a function of solids packing fraction for a 30 particle system undergoing steady shear with $\dot{\epsilon} = 5.0$.

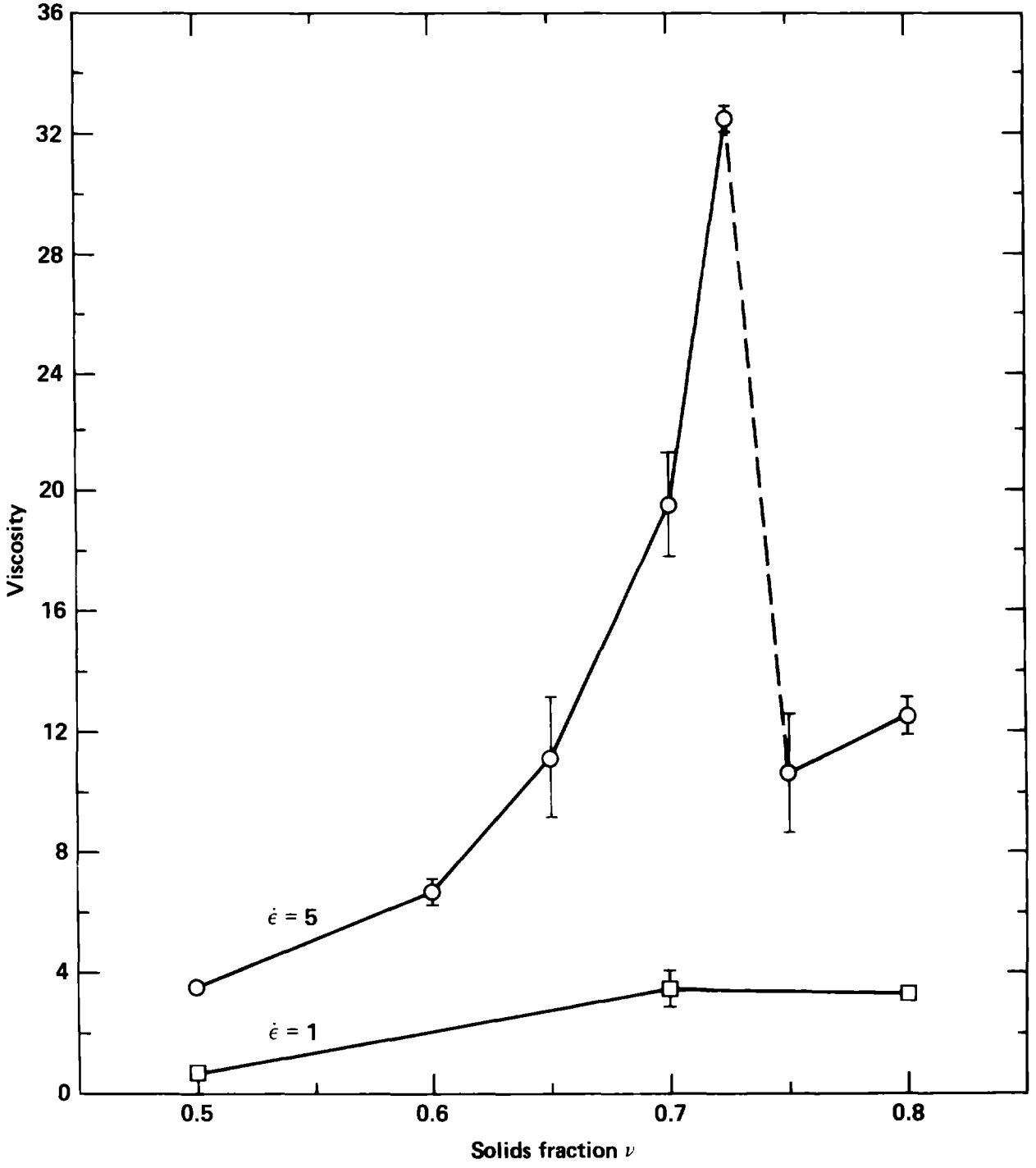

Figure 9. Calculated two-dimensional viscosity, $(p_{xy}+p_{yx})/2\dot{\epsilon}$, as a function of solids packing fraction for a 30 particle system undergoing steady shear with $\dot{\epsilon}$ = 5.0 and $\dot{\epsilon}$ = 1.0.

Errata for Granular Flow Project - Quarterly Report Oct-Dec 84, UCID-20297-84-4

The label on the horizontal axis in Figures 2 and 3 and the lower graph in Figures 5 and 6 should read:

Normal to tangential (translational) velocity ratio, $|v_n|/|v_t|$

Also, the world "scaled" should be eliminated from the captions on Figures 2 and 3.